Innovative Approaches to Improve the Mechanical and Durability Properties of Recycled Aggregate Concrete

Bassam S. A. Dabbour, MZA Mohd Zahid, B.H. Abu Bakar, Abrahem A Ali Blash, Rahman N.A., Herni Halim

***ABSTRACT*- The growing demand for sustainable construction solutions has emphasized the importance of replacing natural aggregates (NA) with recycled aggregates (RA). However, recycled aggregate concrete (RAC) faces challenges such as reduced mechanical strength and durability due to weak residual mortar and an inferior interfacial transition zone (ITZ). This study focuses on enhancing the properties of RAC through acid treatment and the addition of supplementary cementitious materials (SCMs), including silica fume (SF), fly ash (FA), and kaolin (KA). Hydrochloric acid was used to improve the quality of the recycled aggregates, while a two-stage mixing approach (TSMA) was adopted to ensure concrete homogeneity. The use of treated recycled aggregates (TRA) in combination with SCMs led to significant improvements in mechanical properties. For instance, concrete containing 10% SF exhibited a 16.1% increase in compressive strength, a 14.6% increase in flexural strength, and a 12.2% increase in splitting tensile strength. Additionally, the inclusion of SCMs, particularly 10% SF, reduced water absorption by 35.87%, porosity by 40.68%, and rapid chloride permeability by 73.41%, as confirmed by microstructural investigations. These enhancements can be attributed to the ability of SCMs to refine the ITZ, reduce voids, and promote the formation of calcium silicate hydrate (CSH), which contributes to improved durability. Among the SCMs tested, 10% SF demonstrated the most significant improvements in both mechanical and durability properties. Overall, this study concludes that the combination of acid-treated RAC, SCMs, and TSMA provides a sustainable and high-performance alternative to conventional concrete, addressing key challenges while promoting environmental sustainability. To facilitate broader applications in construction projects, its recommendation to further explore the use of hybrid SCM combinations and advanced treatment techniques that allow optimisation of RAC performance.**

***Index Terms*—Recycled Aggregate Concrete, Silica Fume, Fly Ash, Kaolin, Treated Recycled Aggregate, Durability.**

Manuscript received October 26, 2024; revised July 12, 2025.

Bassam S. A. Dabbour is a PhD candidate at the School of Civil Engineering, Kampus Kejuruteraan, Universiti Sains Malaysia, 14300, Nibong Tebal, Pulau Pinang, Malaysia. (e-mail: bassam.dabbour@student.usm.my).

MZA Mohd Zahid is a lecturer at the School of Civil Engineering, Kampus Kejuruteraan, Universiti Sains Malaysia, 14300, Nibong Tebal, Pulau Pinang, Malaysia (Corresponding author; e-mail mohdzulham@usm.my).

B.H. Abu Bakar is a professor in School of Civil Engineering, Kampus Kejuruteraan, Universiti Sains Malaysia, 14300, Nibong Tebal, Pulau Pinang, Malaysia (e-mail: cebad@usm.my).

Abrahem A Ali Blash is a lecturer at the Department of Civil Engineering, College of Engineering Technology - Houn, 61160, Houn, Libya (e-mail:blash1985@gmail.com.; blash2021@student.usm.my).

Rahman N. A is an associate professor at the School of Civil Engineering, Kampus Kejuruteraan, Universiti Sains Malaysia, 14300, Nibong Tebal, Pulau Pinang, Malaysia (E-mail: celindarahman@usm.my).

Herni Halim is a lecturer at the School of Civil Engineering, Kampus Kejuruteraan, Universiti Sains Malaysia, 14300, Nibong Tebal, Pulau Pinang, Malaysia (E-mail: ceherni@usm.my).

I. Introduction

THE increase in global population density has heightened the demand for infrastructure to support modern activities, leading to significant expansion and development in the construction industry over the past two decades. However, this rapid growth has also resulted in a high rate of building demolitions, generating a substantial amount of waste concrete. [1]- [3].

Demolished concrete represents a valuable resource that can be recycled by crushing it into smaller aggregates and removing contaminants [4], [5]. This recycling process offers both environmental and economic benefits, including the reduction of CO_2 emissions and the conservation of natural resources [6], [7]. Economically, recycled concrete (RC) reduces construction costs, minimizes disposal needs, and lessens the demand for virgin materials [6], [8]. RC has a wide range of applications in the construction industry, including its use in new concrete mixes and as a base material for roads [4], [7]. However, the quality of RC can vary, requiring thorough testing and quality control to meet industry standards [2], [8].

Despite the potential benefits of recycled concrete aggregates (RCAs), research reveals some notable gaps. Studies, such as Kim (2024), highlight that the quality of RCAs is inconsistent, with mechanical properties and durability varying significantly based on the material source and processing methods [9]. Furthermore, the long-term behavior of structures made with RCAs remains poorly understood, raising concerns about their durability and structural integrity over time [10]. Additionally, designing concrete mixes that balance sustainability and performance while using recycled materials continues to pose challenges [2].

Globally, concrete waste generation is a pressing issue. For instance, China produces approximately 200 million tons of concrete waste annually, while Australia generates 44 million tons, 37.99% of which originates from building construction and demolition [5]. Concrete rubble from demolished structures can take centuries to decompose, and improper disposal contributes to wasted material and the depletion of valuable land resources. Moreover, it exacerbates the strain on natural aggregate supplies [5].

Studies have shown that RCAs can replace natural aggregates (NAs) partially or entirely in concrete structures. However, RCAs are less effective as a complete replacement due to their inferior characteristics compared to NAs. These include lower specific gravity, higher water absorption, and higher "Los Angeles abrasion" and crushing values, primarily due to the weak mortar that adheres to RCAs [12]-[16]. This

weak mortar reduces the mechanical and durability performance of recycled aggregate concrete (RAC) [17]-[22]. Replacing 50% of NAs with RCAs leads to slump variations ranging from -29% to +17% compared to normal aggregate concrete (NC), while 100% replacement results in variations of -48% to +31%. Concrete density decreases by 1.24% to 4.05% at 50% replacement and by 3.3% to 4.4% at 100% replacement. Additionally, 50% RCA replacement reduces compressive strength, splitting tensile strength, and flexural strength by 4.6% to 19%, 4.9% to 17.5%, and 5% to 24%, respectively. These reductions are more pronounced at 100% replacement, with decreases of 3.6% to 19%, 1.8% to 15%, and 11% to 47%, respectively [18]-[24].

The strength of RAC depends on several factors, including the properties of the original aggregate, the strength of the cement mortar bonding to the aggregate, and the interfacial transition zone (ITZ). In conventional concrete, the ITZ between natural aggregates and mortar is strong, with minimal microcracking until failure occurs in the cement mortar or the ITZ. In RAC, however, the mortar and ITZ are weaker due to pre-existing microcracks formed during the crushing and processing of recycled concrete rubble. These microcracks weaken the bond strength between RCAs and the surrounding mortar, reducing overall material strength [24], [25]. Researchers have explored methods to improve RCA properties, such as treating the aggregates with hydrochloric acid to remove weak mortar [27]-[30]. This treatment reduces water absorption, increases specific gravity, and improves abrasion resistance, thereby enhancing both the compressive and flexural strengths of treated recycled aggregate concrete (TRAC) [11], [26], [29], [30].

Cement hydration produces calcium silicate hydrate (CSH), a compound critical for concrete strength. However, calcium hydroxide (CH), a byproduct of hydration, can leach out, creating voids that weaken compressive strength and reduce durability. CH also reacts with CO_2 to form calcium carbonate ($CaCO_3$) through carbonation, which lowers concrete pH and durability [31], [32]. Supplementary cementitious materials (SCMs), such as silica fume (SF), fly ash (FA), and kaolin (KA), improve concrete strength by reacting with CH to form additional CSH [32], [33], [34]. Studies indicate that SF can consume up to 25% of CH within 28 days, enhancing strength and durability. The pozzolanic activity of SCMs strengthens the ITZ, fills microcracks, and reduces porosity and permeability, thereby improving RAC's mechanical properties [33], [35].

The two-stage mixing approach (TSMA), can further enhance RAC properties. Research shows that replacing 55% to 70% of NAs with RCAs and using TSMA improves compressive strength by 9.13% to 11.93% and flexural strength by 2.4% to 9.38% compared to conventional mixing methods [31], [37]-[39]. Despite these advancements, fully replacing NAs with RCAs remains challenging, with strength and durability still lagging behind those of normal concrete (NC). This study aims to address these limitations by improving the mechanical properties and durability of RAC through the use of SCMs (SF, FA, KA), hydrochloric acid treatment of RCAs, and the application of TSMA in the mixing process.

II. Experimental works

A. Materials

Granite was used as the natural aggregate (NA) in the normal concrete, serving as the control specimen in this study. Treated Recycled Aggregate (TRA) was utilized in the Treated Recycled Aggregate Concrete (TRAC). The Recycled Aggregate (RA) underwent a four-stage treatment process, which is detailed in the subsequent section. Table III summarizes the concrete mix proportions used in this study, consisting of Cement I 52.5 N (OPC), water, river sand (RS), coarse aggregate, and supplementary cementitious materials (SCMs) such as densified silica fume (SF), fly ash (FA), kaolin (KA), and superplasticizer (SP).

1. Granular Aggregate materials

The natural aggregate (NA) used in normal aggregate concrete (NC) consisted of quarry granite with a particle size of 19 mm and a specific gravity of 2.67. Recycled aggregate (RA) was produced by crushing concrete rubble using a machine with a calibrated opening width of 12.5 mm. The crushed material was then sieved through 19 mm and 4.76 mm sieves to remove particles larger than 19 mm and smaller than 4.76 mm. The remaining aggregates, retained between the 19 mm and 4.76 mm sieves, had a maximum particle size of 12.5 mm.

2. Treating Recycled Aggregate materials

RA comprises a mixture of cement mortar (CM) and granite aggregate, with the CM and the interfacial transition zone (ITZ) being the weakest components in normal-strength concretes. During the grinding process to produce RA, cracks often develop in these components, reducing RA's quality. Various treatment methods were applied to improve RA using a 0.1M hydrochloric acid (HCl) solution for one day. These treatments included rinsing, wet washing with a 4.76 mm sieve, acid soaking, carbonation, grinding, and heat treatment. These processes help remove weak mortar and dust.

The HCl treatment significantly improved the compressive and flexural strengths of concrete by 8.44% and 5.51%, respectively, and the splitting tensile strength by 4.92% compared to untreated recycled aggregate concrete [39]. Similarly, Saravanakumar et al. [40] reported a 7.72% increase in compressive strength with a 0.1M HCl treatment. Although the treatment reduced RA's pH by 2.54%, this change did not significantly affect concrete properties [41]. Tanta et al. [14] found that submerging RA in a 0.8M HCl solution for one day improved compressive and splitting tensile strengths by 25.32% and 17.11%, respectively.

The HCl treatment relies on the reaction between HCl and residual mortar bonded to RA. As shown in Equations 1 and 2, HCl reacts with calcium hydroxide ($Ca(OH)_2$), forming soluble calcium chloride ($CaCl_2$) and dissolving hydrated calcium silicate (CSH), which are key constituents of cement mortar. This process removes weak surface mortar, exposing a clean, rough surface that enhances the bond between fresh mortar and RA. However, excessive HCl concentration or prolonged immersion can increase voids and porosity, thereby weakening the aggregate and reducing the quality of both RA and RAC [42], [43].

$$Ca(OH)_2 + 2HCL \rightarrow CaCL_2 + 2H_2O \quad (1)[42], [43]$$

$$xCaO.ySiO_2.nH_2O + 2xHCL \rightarrow xCa^{2+} + 2xCL^{-1} + ySi(OH)_4 + (x + n - 2y)H_2O \quad (2)\ [42], [43]$$

In this study, RA was treated with 0.1M HCl at pH 1. The treatment process involved five steps:

1. Rinsing RA with water through a 4.76 mm sieve to remove dust and small particles.
2. Submerging RA in HCl for one day.
3. Rinsing RA to eliminate residual HCl.
4. Air-drying RA to achieve a saturated surface-dry state.
5. Sieving RA through a 4.76 mm sieve to remove decomposed mortar.

A scanning electron microscope (SEM) analysis was performed on RA samples before and after treatment at the Earth Material Characterization Laboratory, Archaeology Department, Universiti Sains Malaysia. Figure 1(a) illustrates untreated RA with cement mortar adhered to the natural aggregate and visible cracks in the ITZ. In contrast, Figure 1(b) shows treated RA (TRA) with a clean, rough surface, free of cracks, and significantly reduced weak mortar. The presence of calcium silicate hydrate (CSH) and calcium hydroxide (CH) in the treated RA indicates successful treatment.

3. Physical Properties of Coarse and Fine Aggregates

Mechanical sieving was conducted in accordance with ASTM C33 for NA and TRA, and ASTM C136 for RS and the results as illustrated in Figure 2. Table I presents the results for RS, NA, and TRA alongside their specified limits. The fineness modulus of RS was recorded as 3.08. Table I also summarizes the physical properties, including unit weight, specific gravity, and absorption values. The absorption values were 0.41% for NA, 4.89% for RA, and 4.4% for TRA. HCl treatment reduced TRA absorption by 10% compared to RA, thereby enhancing TRA's physical properties.

4. Cementitious materials

This study used Ordinary Portland Cement (OPC), classified as CEM I, 52.5 N, and SCMs such as densified silica fume (SF), fly ash (FA), and kaolin (KA). Table II provides the chemical compositions of these materials. SEM imaging Figure 3 was utilized to examine the morphology and structure of OPC, FA, KA, and SF. ImageJ software was used to analyze SEM images and measure particle dimensions.

The OPC particles exhibited a non-uniform cross-sectional shape with a rough texture. The particle size ranged from 1 µm to 100 µm, with over 90% of the particles being smaller than 10 µm. SF particles ranged between 10 and 250 µm in size, with 72% being smaller than 100 µm, and exhibited a smooth, spherical structure. FA had a particle size distribution between 1 and 2 µm, with 93.2% of particles smaller than 5 µm, and displayed a smooth, rounded structure. SEM analysis revealed that KA particles ranged from 4 to 30 µm, with over 68% being smaller than 10 µm, and had a rough, irregular surface.

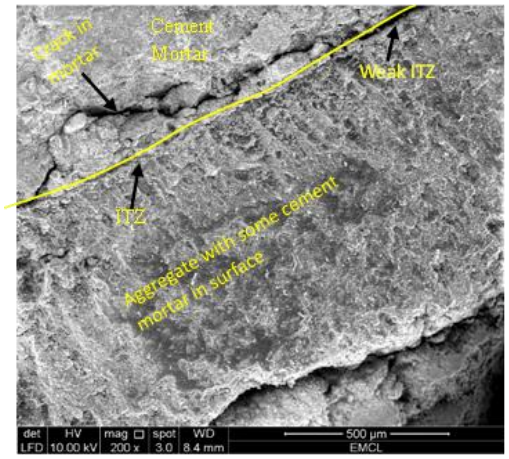

(a) Untreated recycled aggregate

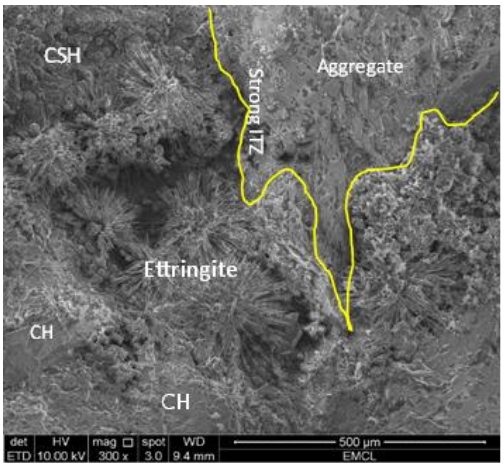

(b) Treated recycled aggregate

Fig. 1. The result of scanning electron microscope (SEM) for the untreated and treated recycled aggregate.

TABLE I
CHARACTERISTICS OF MATERIALS USED (RIVER SAND, NATURAL AGGREGATE, RECYCLED AGGREGATE, TRA & THE RECYCLED AGGREGATE TREATMENT EFFECT)

Analysis Type(s)	Required Analysis	Material				
		RS	NA	RA	TRA	Effect of RA treatment
Max. size (mm)	ASTM C136	4.76	19	19	12.5	-
Min. size (mm)		0.076	2.36	2.36	4.76	-
Flakiness (%)	BS 812-105.1	-	10.7	6.2	8.8	-41.9%
Elongation (%)	BS 812-105.2	-	17	19.4	14.0	+27.8%
BSG (-)	ASTM C128	2.581	2.648	2.317	2.351	
BSG (SSD) (-)		2.607	2.659	2.431	2.428	
ASG (-)		2.649	2.677	2.614	2.546	
ABS (%)		0.99	0.41	4.89	4.4	-10.0%
UW (Kg/m³)	ASTM C29	1.586	1.447	1.232		
CV (%)	BS 812-110:1990	-	22.12	29.05	27.51	-5.3%
LA (%)	ASTM C131	-	25.00	37.44	33.64	-10.0%

Acronyms: ABS: Absorption, ASG: Apparent specific gravity, BSG (SSD): Bulk specific gravity SSD condition, BSG: Bulk specific gravity, CV: Crushing value, LA: Los Angeles, UW: Unit weight.

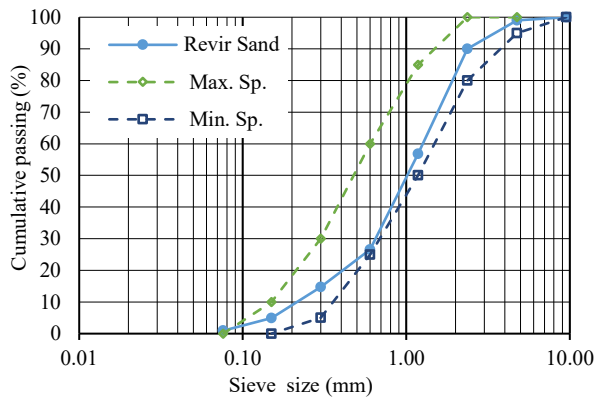

(a) River sand

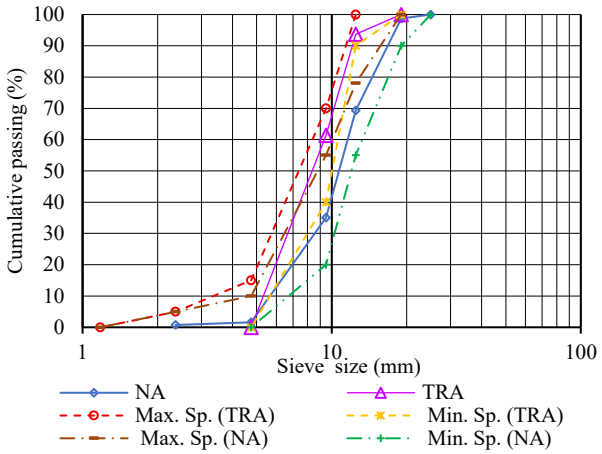

(b) Natural and treated recycled aggregate.

Fig. 2. The sieve analysis of concrete ingredients, and their respective specification limits.

B. Mixing Procedure

This study employed the two-stage mixing approach (TSMA) [38], [44], as depicted in Figure 4. This method involves two distinct mixing stages followed by the casting phase, with a total duration of 12 minutes. The first stage, lasting 4 minutes, begins with the addition of coarse aggregates to the mixing container. These aggregates are dry mixed to ensure uniform distribution. Fine materials, such as sand or powdered substances, are then gradually introduced, followed by the addition of water. The mixture is thoroughly blended to form a uniform base material that serves as the foundation for the second stage.

The second stage, which takes 8 minutes, starts with the addition of more water to achieve the desired workability of the mix. A chemical additive, such as a superplasticizer, is then introduced to enhance specific concrete properties, such as strength, durability, and workability. The mixture is further homogenized through thorough mixing, ensuring even distribution of the additives and achieving the required consistency for casting. This stage completes the preparation of the concrete mix.

The final phase is casting, where the prepared concrete is poured into molds. Tools, such as tamping rods and slump cones, are used to compact the mix, eliminate air voids, and ensure the molds are properly filled. Once the molds are prepared, the concrete is left to cure, allowing it to gain strength and durability over time. The TSMA process, as depicted in the figure 4, is designed to optimize the quality of concrete by systematically introducing materials and additives, resulting in a homogeneous and high-performance mix suitable for construction applications.

TABLE II:
CHEMICAL CHARACTERISTICS OF USED CEMENT, DENSIFIED, FLY ASH, KAOLIN & SILICA FUME

Oxide(s)	Cement	Densified silica fume	Fly ash	Kaolin
Silicon dioxide (SiO_2)	19.49	95.60	54.40	54.33
Aluminum (Al_2O_3)	5.01	0.27	25.01	30.23
Iron (III) oxide (Fe_2O_3)	3.59	0.07	6.16	1.72
Calcium oxide (CaO)	64.29	0.1	5.53	0.013
Magnesium oxide (MgO)	1.99	0.32	1.54	1.47
potassium oxide (K_2O)	0.56	0.63	1.30	5.63
Sodium oxide Na_2 O	0.11	0.37	0.69	0.08
Titanium (III) oxide (TiO_3)	0.00	0.00	1.22	0.72
Phosphorus pentoxide (P_2O_5)	0.03	0.07	0.87	0.02
Manganese oxide (MnO)	0.01	0.00	.01	0.00

C. Percentage of Supplementary cementitious materials (SCMs)

Previous studies have suggested incorporating 10-15% silica fume (SF) by weight of cement as the optimal range for cement replacement. However, the variations in concrete performance within this range are minimal. Therefore, in this study, SF was added at 10% of the cement weight, aligning with recommendations from prior research [45]-[50]. Similarly, the maximum recommended fly ash (FA) content for cement replacement is 35% by mass [14], with 15% identified as the optimal percentage based on previous findings [51]-[54].

The use of kaolin (KA) in concrete is less common, as most research focuses on metakaolin, which is produced by heating kaolin to 700°C for 3 to 4 hours—a process that demands significant energy. In this study, KA was used as an additive at 5% of the cement weight, which is considered the optimal percentage according to prior research [55]-[58].

D. Design mix proportions

Furthermore, the ACI 211.1 concrete mix design guidelines were adopted to determine the proportions of concrete components, with special emphasis on the absolute volume methodology [59]. In addition to cement, silica fume (SF), fly ash (FA), and kaolin (KA) were incorporated as cement substitutes. Table III provides an overview of the materials used for five different concrete mix designs. The natural aggregate (NA) was used in a completely dry state, while the treated recycled aggregate (TRA) was utilized in a saturated surface-dry condition.

E. Specimens' preparation, casting, and curing

Concrete cube molds measuring 100 mm x 100 mm x 100 mm were used to prepare specimens for testing compressive strength, water absorption, porosity, and density [59], [60]. While cylindrical molds with a diameter of 100 mm and a height of 200 mm were used to prepare concrete specimens for evaluating the modulus of elasticity and splitting tensile strength. Flexural strength was determined using prism molds measuring 100 mm × 100 mm × 400 mm [60], [61]. For water permeability testing, cylindrical samples measuring 50 mm in diameter and 40 mm in height were prepared. To evaluate rapid chloride permeability (RCP), cylindrical specimens with dimensions of 100 mm in diameter and 50 mm in height

were used [62]. A vibration table was employed to ensure effective compaction of the concrete mixes, and after that a slump test was conducted. The prepared samples were stored at a temperature range of 23–30°C, with damp cloths placed over them for 24 hours. After this initial curing period, the samples were demolded and placed in a controlled curing water tank maintained at 23–27°C. The specimens were cured and tested at different intervals: the 7th, 28th, 56th, and 96th days [63].

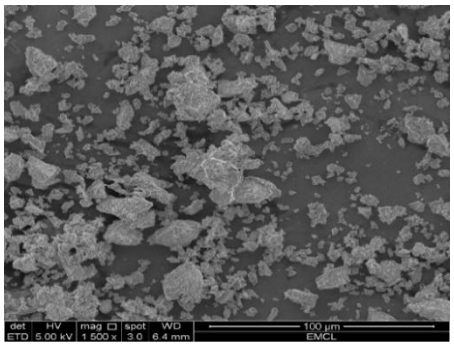

(a) Cement (OPC).

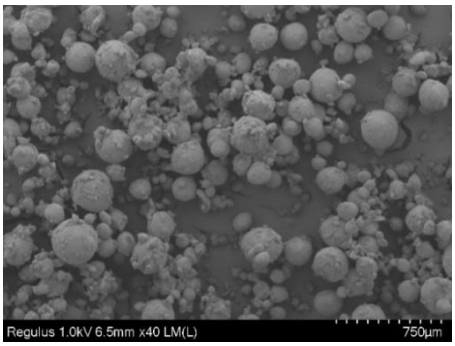

(b) Silica fume (SF).

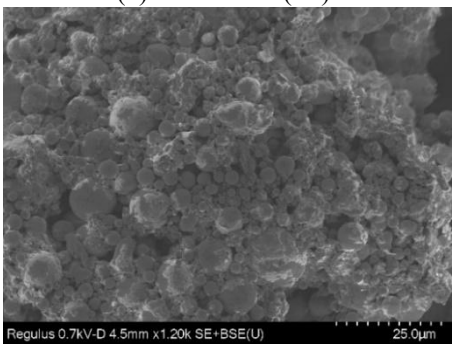

(c) Fly ash (FA).

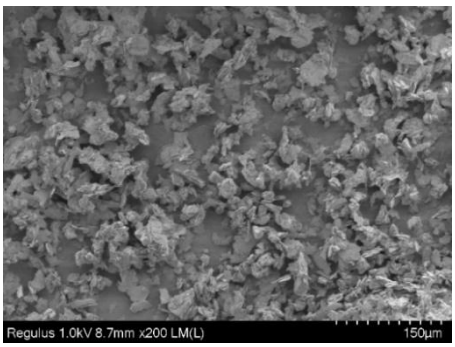

(d) Kaolin (KA)

Fig. 3. Scanning Electron Microscope (SEM) images for supplementary cementitious materials

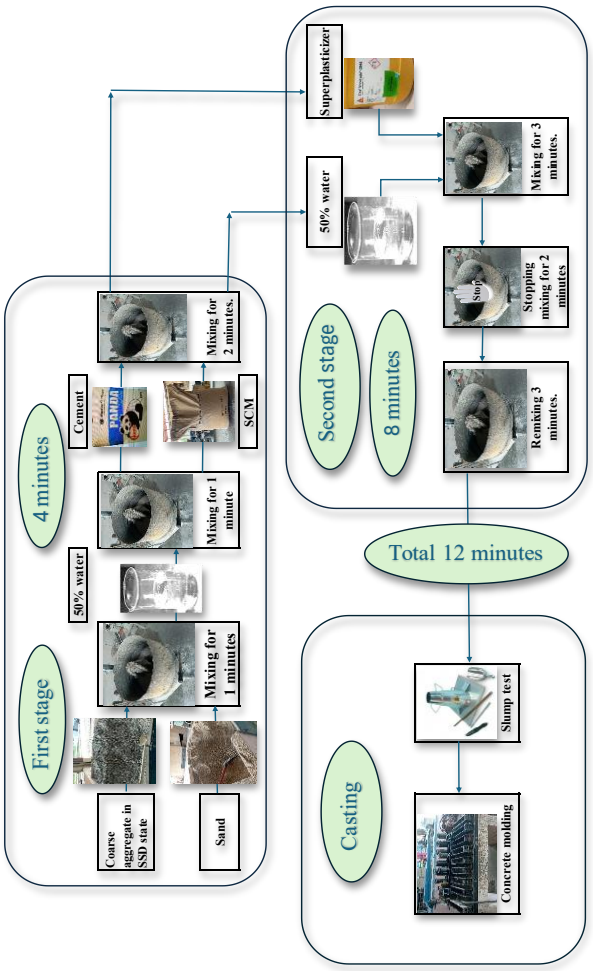

Fig. 4. Flow process of concrete mixing using two-stage mixing approach (TSMA).

TABLE III
CONVENTIONAL PROPORTIONS OF MIXING BOTH CONCRETE AND TRAC

Material	Units	Mix name				
		NC	TRAC1	TRAC2-SF10	TRAC3-FA15	TRAC4-KA5
Cement	Kg/m^3	444	444	444	444	444
W for W/C	Kg/m^3	200	200	200	200	200
W for SCMs	Kg/m^3	0	0	20	30	10
Addition of water for aggregate absorption	Kg/m^3	11	7	7	7	7
Total water	Kg/m^3	211	207	227	237	217
River sand	Kg/m^3	770	680	680	680	680
Coarse aggregates	Kg/m^3	900	940	940	940	940
Silica fume	Kg/m^3	-	-	44.4	-	-
Fly ash	Kg/m^3	-	-	-	66.6	-
Kaolin	Kg/m^3	-	-	-		22.2
Superplasticizer	Kg/m^3	-	-	2.2	2.2	2.2
	(%)	-	-	0.5	0.5	0.5

Acronyms: “NC – normal concrete containing granite aggregate; TRAC – concrete with TRA; the numerical values of N and TRAC are the sequential job mix numbers; the numbers following SF, FA, and KA are the proportions of material added to the concrete mix; CA – coarse aggregate; Wc – water quantity for total cementitious material”.

F. Wet and hardened concretes testing

Concrete workability test

The slump test, conducted in accordance with ASTM C143 standards [64], [65], was performed to assess the workability of the concrete.

Density, Absorption, and Porosity

The saturated surface dry density (ρ_{SSD}), absorption (ABS), and porosity (n) were determined in accordance with ASTM C642 guidelines, using Equations (3)–(5) [66].

$$\rho_{SSD} = \frac{W_{SSD}}{W_{SSD} - W_{SUB}} * \rho_W \quad (3)$$

$$ABS = \frac{W_{SSD} - W_D}{W_D} * 100\% \quad (4)$$

$$n = \frac{W_{SSD} - W_D}{W_{SSD} - W_{SUB}} \quad (5)$$

where, ρ_{SSD} is the saturated and surface dry density (g/cm³), W_{SSD} is the weight of sample in SSD condition in the air (g), , W_{sub} is the weight of sample underwater (g), ABS is the water absorption (%), W_D is the weight of sample in dry condition (g), and n is the concrete porosity"

Permeability of Concrete

An innovative method for evaluating concrete's gas and water permeability, developed by researchers Cabrera and Lynsdale, was employed in this study [67][68]. Figure 5 provides an outline of the apparatus used for the permeability test, which includes a permeability cell, a nitrogen gas source, a pressure gauge, and connecting tubes. The calculations for permeability are detailed in Equations (6) and (7) [68].

$$n = \frac{Mf - Md}{\rho * d * \frac{\pi * D^2}{4}} \quad (6)\ [68]$$

$$K = \frac{d^2 * n}{2 * T * h} \quad (7)[68]$$

where, n is concrete porosity, D is the sample diameter (50 mm), K is concrete permeability (m/s), d is water penetration depth, Md is the weight of dry sample (g), T is the time under pressure (3 hours), Mf is the weight of the sample after the test (g), h is applied gas pressure (3bar = 30 m), and ρ is water density (1g/cm³).

Rapid Chloride Permeability (RCP) Test

The Rapid Chloride Permeability (RCP) test, conducted in accordance with ASTM C1202 and AASHTO T259 standards, is a widely accepted method for evaluating the resistance of concrete samples to chloride ion (Cl^-) penetration and reactivity, providing valuable insights into the material's durability. For this study, three cylindrical specimens with dimensions of 102 mm in diameter and 51 mm in height were prepared and cured. These specimens were subsequently tested on the 28th and 96th days [62]. The RCP test measures the total electrical charge passed through the concrete over a 6-hour period, offering a quantitative assessment of its permeability.

(a) Permeability test setup.

(b) Permeability cell.

(c) Concrete specimen fixed within the permeability cell.

Fig. 5. Permeability test setup and accessories.

Compressive Strength(σ_{CU})

The compressive strength of the concrete (σ_{CU}) was measured on the 7th, 28th, 56th, and 96th days using 100 mm cube samples [69], in accordance with BS 1881: Part 116. The compressive strength (σ_{CU}) was calculated using Equation (8).

$$\sigma_{CU} = \frac{P}{A} \quad (8)$$

where, P is the crushing force (N), and A is the spacemen loaded area in mm².

Splitting Tensile Strength

The splitting tensile strength (σsp) of concrete samples was tested on the 28th day of curing, in accordance with ASTM C496 [70]. The splitting tensile strength of the cylindrical samples was calculated using the formula specified in Equation (9).

$$\sigma_{SP} = \frac{2 * P}{\pi * D * L} \quad (9)$$

where, P is the fractured load, D is the sample diameter, and L the sample overall length.

Modulus of Elasticity

The static modulus of elasticity (Ec), cylindrical compressive strength (σcy), and Poisson's ratio (ν) were all evaluated on the 28th day of curing in accordance with ASTM C469 [71]. Two strain gauges were attached to the samples to measure both vertical and transverse strains. The calculations were performed using Equations (10) to (12). Figure 6 illustrates the testing machine components and the tested sample.

$$\sigma_{CY} = \frac{4 * F * P}{\pi * D^2} \tag{10}$$

$$Ec = \frac{\sigma_{40\%} - \sigma_{0.00005}}{\varepsilon_{v_{\sigma 40\%}} - 0.000050} \tag{11}$$

$$\nu = \frac{\varepsilon_{h_{\sigma 40\%}} - \varepsilon_{h_{\sigma 0.00005}}}{\varepsilon_{v_{\sigma 40\%}} - 0.000050} \tag{12}$$

where, F is the correction factor is equal to 1 when the ratio of length to diameter (L/D) is 2, $\sigma_{40\%}$ is the stress value corresponds to 40% of the highest stress during the initial loading stage, $\varepsilon_{v_{\sigma 40\%}}$ is the vertical strain value at 40% of the maximum stress, $\sigma_{0.00005}$ is the stress value induces a vertical strain of 0.00005, $\varepsilon_{h_{\sigma 40\%}}$ is the transverse strain at mid-height of the specimen produced by 40% of the maximum stress, $\varepsilon_{h_{\sigma 0.00005}}$ is the transverse strain at mid-height of the specimen produced by $\sigma_{0.00005}$.

(a) Main frame

(b) Strain gauges, sample fixation, steel load plates and the loading cell

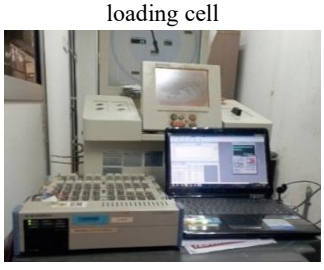

(c) Output system, processing unit, data output, and the transformer.

Fig. 6. Universal Testing Machine (UTM) with a maximum capacity of 1000 kN.

Flexural Strength

Flexural strength (σ_{FL}) was tested on the 28th day in accordance with ASTM C78 standards [60]. The test was conducted using a Universal Testing Machine (UTM) with a load-bearing capacity of 100 kN, as illustrated in Figure 7. The flexural strength was calculated using Equation (13).

$$\sigma_{FL} = \frac{P * L}{B * D^2} \tag{13}$$

Where, P is the maximum flexural load, L is the span length between the supports, B is the samples width, and D is the samples height.

(a) Flexural test setup

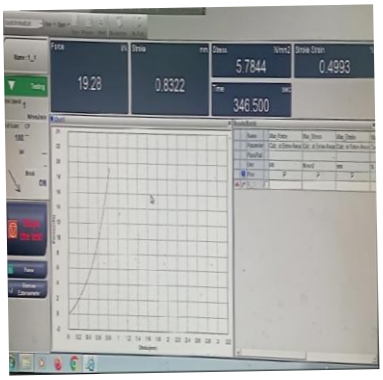

(b) Machine program with visual/output monitor.

Fig. 7. Universal Testing Machine (UTM) with 100 kN capacity.

III. Results and Discussion

A. Slump

The slump values of fresh concrete for each design mix were recorded immediately after mixing, with all five mixes exhibiting a true slump shape. The results are presented in Figure 8. The TRAC1 mix, in which Treated Recycled Aggregate (TRA) replaced Natural Aggregate (NA), showed a slump value 41.7% higher than that of normal concrete (NC). Specifically, TRAC1 achieved a slump of 120 mm compared to 70 mm for NC. Previous studies have shown that replacing 100% NA with RA can increase workability by 31% [21]. The present study demonstrates a higher improvement rate, primarily attributed to the inclusion of 0.5% superplasticizer (SP) and the well-graded, smooth-edges TRA, as shown in Figure 9.

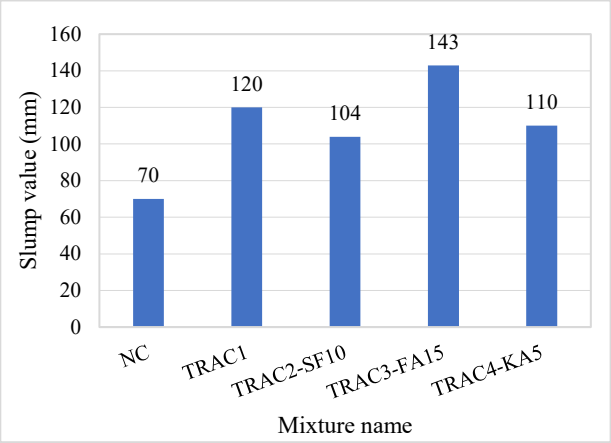

Fig. 8. Slump test results.

In contrast, the TRAC2-SF10 mix, which included 10% silica fume (SF), exhibited a 13.3% decrease in slump compared to TRAC1. Adding SF to concrete mixes can decrease the slump value due to its larger surface area than cement. As SF is added as additional material, the total surface area of the cementitious materials increases, leading to a higher water demand as the extra surface area absorbs more water. This absorption reduces the free water in the concrete mix, resulting in a lower slump value [72], [73], [74].This observation aligns with findings by Köksal et al. [75], which also noted reduced workability with the addition of SF. On the other hand, the incorporation of 15% fly ash (FA) in the TRAC3-FA15 mix improved workability by 19.2% compared to TRAC1. FA has fine particles, different sizes, and spherical and smooth surfaces. The FA's ability to absorb water was less than the densified SF, where the FA with water will work as lubrication and allow sliding for concrete particles, which will increase the concrete workability [76], [77]. However, adding 5% kaolin (KA) in the mix reduced the slump by 8.3%. The lower slump with KA is attributed to its small, irregularly shaped particles, which increase friction between particles, as observed in the SEM images shown in Figure 3(d). This finding is consistent with studies by Kararas et al. [58] and Lotfy et al. [78].

Fig. 9. The smooth edges of TRA.

B. Absorption (ABS), permeability (K), and porosity (n):

Five design mixes were evaluated on the 28th day to determine their absorption (ABS), porosity (n), and permeability (K). The results are summarized in Table IV. The TRAC1 mix exhibited an absorption rate of 4.82%, which was 10.88% higher than that of the NC mix. The difference in ABS between NC and TRAC was not significant due to the pretreatment of RA, which involved washing with water and immersion in HCl. This process effectively removed the weakly adhered mortar, as confirmed by SEM imagery in Figure 1.b. Additionally, the two-stage mixing approach enhanced the concrete's structural densification, as demonstrated by the compact, low-void structure of TRAC1 depicted in Figure 10a. Although the structural densification of TRAC was improved, TRAC1 still showed significantly higher porosity (+28.15%) and permeability (+39.61%) compared to NC. These elevated values likely result from microcracks induced during the mechanical crushing and grinding of concrete debris. As shown in Table IV, TRAC1 is identified as the reference mixture. Notably, the incorporation of 10% SF, 15% FA, or 5% KA significantly reduced ABS, n, and K. For example, the addition of 10% SF resulted in decreases of 35.87% in absorption, 40.68% in porosity, and 73.41% in permeability compared to TRAC. These improvements stem from pozzolanic reactions between the SCMs and calcium hydroxide, facilitating the formation of calcium silicate hydrate. This reaction effectively enhances the matrix's density by filling internal voids and sealing microcracks, as shown in Figure 10.

TABLE IV
ABSORPTION, PERMEABILITY AND POROSITY

Mixtures name	ABS (%)	ΔABS (%)	n (%)	Δn (%)	K $*10^{-11}$ (m/s)	ΔK (%)
NC	4.32	-9.81	9.20	-21.97	2.07	-28.37
TRAC1	4.79	0	11.79	0.00	2.89	0
TRAC2-SF10	3.10	-35.28	6.99	-40.71	0.78	-73.01
TRAC3-FA15	3.87	-19.21	8.59	-27.14	1.09	-62.28
TRAC4-KA5	4.10	-15.41	9.19	-22.05	1.60	-44.64

C. Rapid chloride permeability (RCP) test:

The results of the Rapid Chloride Permeability (RCP) tests conducted on the concrete specimens at 28 and 96 days of curing are presented in Figures 11 and 12, respectively. For normal concrete (NC), the RCP value was recorded as 4557 Coulombs (classified as high) at 28 days and 3449 Coulombs (moderate) at 96 days, indicating improved cement hydration over time. In comparison, TRAC1 exhibited higher RCP values at both ages, with 6029 Coulombs at 28 days and 4868 Coulombs at 96 days. This increase is attributed to its higher absorption (ABS), porosity, and permeability.

Incorporating supplementary cementitious materials (SCMs) significantly reduced RCP values. For instance, adding 10% silica fume (SF) in TRAC2-SF10 decreased RCP values by 78.3% at 28 days and 80.8% at 96 days. Similarly, the TRAC3-FA15 mix, containing 15% fly ash (FA), saw reductions of 45.9% at 28 days and 53.3% at 96 days. Adding 5% kaolin (KA) to TRAC4-KA5 reduced RCP by 34.8% and 41.9% at 28 and 96 days, respectively. These reductions are attributed to the pozzolanic reactions of SF, FA, and KA with calcium hydroxide (CH), which produce additional calcium silicate hydrate (CSH), enhancing the concrete's microstructure. This is further supported by the SEM images presented in Figure 10.

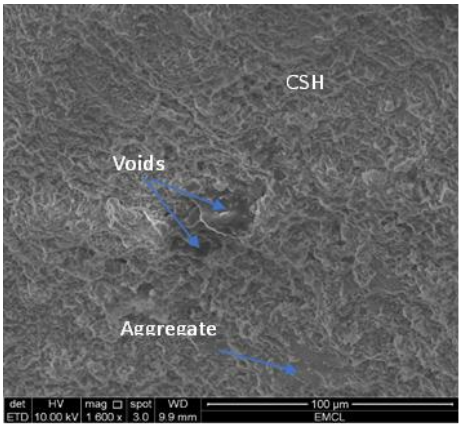

(a) SEM image explains dense concrete without visible microcracks or visible voids in TRAC1.

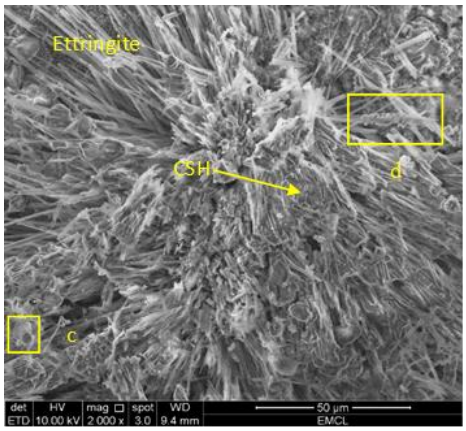

(b) SEM image shows the presence of CSH, CH, SCMs.

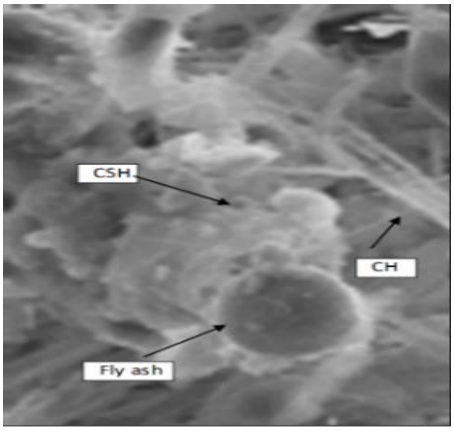

(c) SEM image shows the reaction of FA and CH and the formation of CSH.

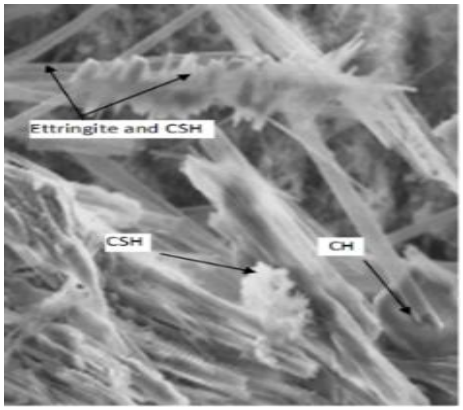

(d) SEM image shows the development of CSH resulting from the reaction between SCM and CH

Fig. 10. SEM image results for concrete samples

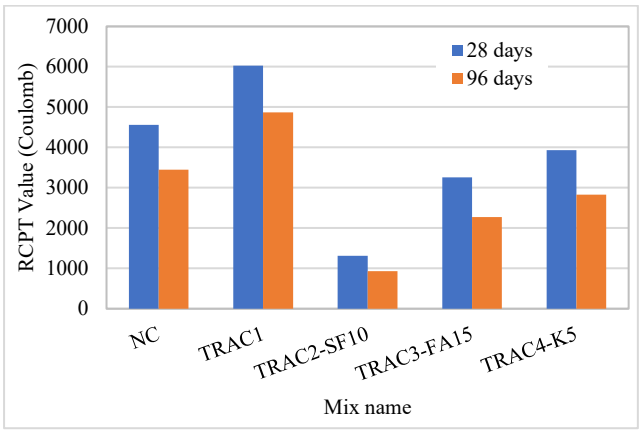

Fig. 11. The result of the rapid chloride permeability (RCP).

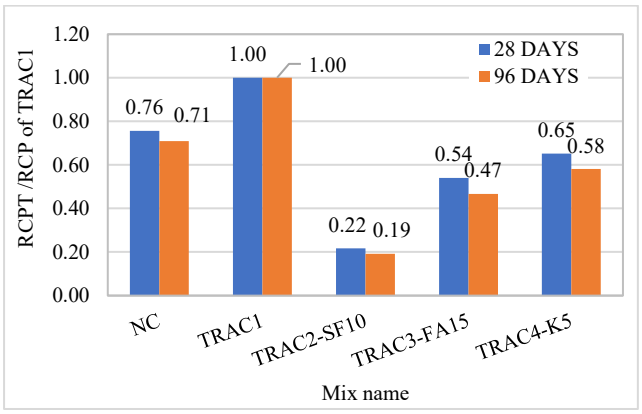

Fig. 12. Comparison of RCP results with respect to TRAC1

D. The Relationship between permeability (K), absorption (ABS), and porosity (n) with RCP

The relationships between Rapid Chloride Permeability (RCP) values and key concrete properties, including absorption, porosity, and permeability, are illustrated in Figures 13(a), 13(b), and 13(c), respectively. These relationships demonstrate strong linear correlations, underscoring the significance of these properties in influencing chloride ion penetration and concrete durability.

Figure 13(a) presents the correlation between absorption (%) and RCP values (Coulombs). The data exhibits a clear linear trend, where higher absorption levels correspond to increased RCP values. This relationship is expressed by Equation (14).

$$RCP = 2726.9 * ABS - 7173.8 \quad (14)$$

The coefficient of determination ($R^2 = 0.9985$) indicates an exceptionally strong linear correlation, confirming the model's accuracy in predicting RCP values based on absorption. The positive slope suggests that increased absorption, driven by higher porosity, significantly contributes to greater chloride ion permeability. Reducing absorption is therefore critical for enhancing concrete's durability and resistance to chloride penetration.

Figure 13(b) illustrates the relationship between porosity (%) and RCP values (Coulombs). A positive linear correlation is observed, indicating that as porosity increases, RCP values also rise. This relationship is defined by Equation (15):

$$RCP = 966.54 * n - 4759.8 \quad (15)$$

where n represents porosity. The coefficient of determination ($R^2 = 0.9345$) shows a strong correlation, with 93.45% of the variation in RCP values explained by porosity. Higher porosity levels create pathways for chloride ion ingress, increasing vulnerability to corrosion. Minimizing porosity through effective design and the use of supplementary cementitious materials (SCMs) is essential to improve concrete's resistance to chloride penetration and enhance long-term durability.

Figure 13(c) explores the relationship between permeability (m/s × 10^{-11}) and RCP values (Coulombs). The data reveals a strong positive linear correlation, indicating that higher permeability results in greater RCP values. This relationship is represented by Equation (16):

$$RCP = 1979.1 * K + 454.7 \quad (16)$$

where K is permeability. The coefficient of determination ($R^2 = 0.9211$) highlights the model's reliability, with 92.11% of the RCP variation attributed to permeability. High permeability, often associated with increased porosity and micro-cracks, facilitates chloride ion penetration, reducing durability. Reducing permeability by incorporating SCMs such as silica fume, fly ash, and kaolin enhances the concrete microstructure by filling voids and sealing micro-cracks, as demonstrated in this study. Lower permeability improves resistance to chloride ingress, minimizing the risk of corrosion in reinforced concrete and extending its service life.

Figures 13(a), 13(b), and 13(c) emphasize the importance of controlling absorption, porosity, and permeability to improve concrete durability. These findings highlight the role of SCMs in refining the concrete matrix and reducing these properties, thereby significantly enhancing resistance to chloride penetration and promoting long-term performance.

E. Concrete compressive strength (σ_{cu})

The compressive strength (σ_{cu}) tests were conducted on the 7th, 28th, 56th, and 98th days of curing, with the results summarized in Table V and illustrated in Figure 14. On the 7th day, TRAC1 exhibited a compressive strength of 40.5 MPa, which increased to 54.1 MPa by the 98th day of curing. This represents a reduction of less than 5% compared to normal concrete (NC). The minimal reduction can be attributed to the removal of old mortar and the use of well-graded treated recycled aggregate (TRA) during the crushing and treatment process. This finding aligns with Saravakumar et al. [40], who reported a 34.6% increase in compressive strength when using HCl-treated recycled aggregate compared to untreated recycled aggregate.

The incorporation of 10% silica fume (SF) or 15% fly ash (FA) significantly enhanced the compressive strength of TRAC2-SF10 and TRAC3-FA15. On the 28th day, TRAC2-SF10 showed a 16.1% increase in compressive strength, while TRAC3-FA15 exhibited a 10.8% increase compared to TRAC1. Further strength gains were observed at 56 and 98 days. These improvements are attributed to pozzolanic reactions between calcium hydroxide (CH) and the silica in SF and FA, which form calcium silicate hydrate (CSH). The formation of CSH strengthens the concrete matrix and improves overall durability.

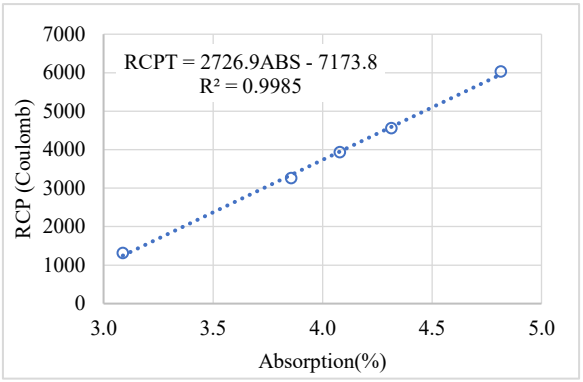

(a) ABS-RCP relation

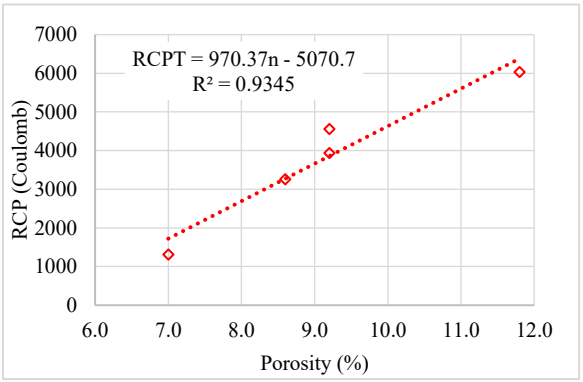

(b) n-RCP relation

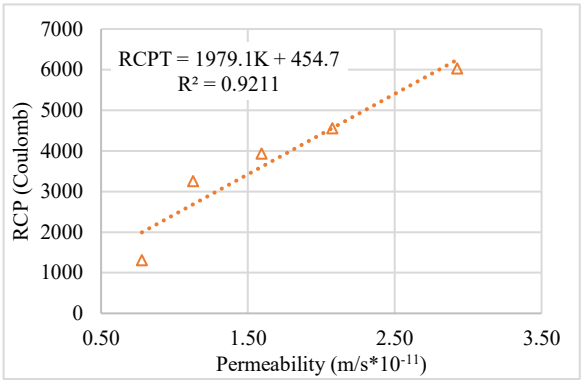

(c) K-RCP relation

Fig. 13. Correlations between permeability, water absorption, & porosity, in respect of RCP.

TABLE V
COMPRESSIVE STRENGTH AND PERCENTAGE DIFFERENCE WITH RESPECT TO TRAC1.

Mix design Codes	7th day		28th day		56th day		98th day	
	σ_{cu} (MPa)	$\Delta\sigma_{cu}$ (%)	σ_{cu} (MPa)	$\Delta\sigma_{cu}$ (%)	σ_{cu} (MPa)	$\Delta\sigma_{cu}$ (%)	σ_{cu} (MPa)	$\Delta\sigma_{cu}$ (%)
NC	42.4	4.7	51.4	4.7	54.2	4.2	56.3	4.1
TRAC1	40.5	0.0	49.1	0.0	52.0	0.0	54.1	0.0
TRAC2-SF10	47.4	17.0	57.0	16.1	60.0	15.4	61.7	14.0
TRAC3-FA15	44.2	9.1	54.4	10.8	58.0	11.5	62.0	14.6
TRAC4-KA5	43.0	6.2	52.3	6.5	55.67	7.1	58.0	7.2

F. Concrete splitting tensile strength

The splitting tensile strength (σ_{sp}) was tested after 28 days of curing, with the results presented in Figure 15(a). TRAC1 exhibited splitting tensile strength nearly identical to NC,

with a difference of only 1.78%. The addition of 10% silica fume (SF), 15% fly ash (FA), and 5% kaolin (KA) increased the splitting tensile strength by 12.21%, 6.87%, and 5.09%, respectively. These improvements align with findings from previous studies [46], [74]-[76] and are attributed to the formation of calcium silicate hydrate (CSH), which fills voids and strengthens the bonding within the cement paste and treated recycled aggregate (TRA).

Figure 15(b) illustrates the relationship between compressive strength (MPa) and splitting tensile strength (MPa) for treated recycled aggregate concrete (TRAC). A strong positive correlation is observed, indicating that as compressive strength increases, splitting tensile strength also increases and the relationship is expressed by equation 17.

$$\sigma_{sp} = 0.191 * \sigma_{cu}^{0.776} \quad (17)$$

Where, σ_{sp} represents splitting tensile strength, and σ_{cu} is compressive strength.

The trendline fits the data well, as shown by the R^2 value of 0.9702, indicating that 97.02% of the variation in splitting tensile strength can be explained by the compressive strength. The data points form a clear upward trend, signifying that higher compressive strength corresponds to higher splitting tensile strength. This is expected as both properties are related to the internal bonding and strength of the concrete matrix. The graph demonstrates that splitting tensile strength increases at a slower rate compared to compressive strength, as indicated by the power exponent (0.7762). This aligns with the typical behavior of concrete, where tensile strength is lower than compressive strength but follows a predictable relationship.

The high R^2 value suggests that the model is highly reliable for predicting splitting tensile strength based on compressive strength for TRAC. These findings emphasize the importance of optimizing compressive strength through the use of supplementary cementitious materials and proper aggregate treatment to achieve superior overall mechanical performance.

G.Modulus of elasticity (E_c):

The results from the Table VI indicate that the incorporation of supplementary materials in concrete mixes influences both the compressive strength and the modulus of elasticity. Among the mixes, TRAC2-SF10 exhibits the highest compressive strength of 45.6 MPa and the highest modulus of elasticity at 33,120 MPa. This suggests that the addition of silica fume (SF10) enhances the mechanical properties significantly, achieving a 9.95% improvement in the modulus of elasticity compared to the reference mix, TRAC1. On the other hand, the control mix (NC) recorded a compressive strength of 43.0 MPa and a modulus of elasticity of 32,989 MPa, slightly lower than TRAC2-SF10, indicating the positive effect of material modification.

The mix TRAC1, which serves as the baseline, shows the lowest values in both compressive strength (41.2 MPa) and modulus of elasticity (30,122 MPa), with no observed improvement in elastic properties. Other mixes, such as TRAC3-FA15 and TRAC4-KAS, demonstrate moderate enhancements. For example, TRAC3-FA15, with 15% fly ash, shows a compressive strength of 44.8 MPa and a modulus of elasticity of 31,654 MPa, reflecting a 5.09% increase in elastic modulus. Similarly, TRAC4-KAS exhibits a compressive strength of 43.7 MPa and a modulus of elasticity of 31,698 MPa, resulting in a 5.23% improvement in elasticity.

Overall, the findings highlight the potential of treated recycled aggregate (TRAC) as a sustainable alternative to natural aggregate, especially when combined with supplementary cementitious materials. Although TRAC1 (without supplementary materials) showed lower performance than normal concrete, the addition of silica fume in TRAC2-SF10 not only overcame this deficit but also achieved superior mechanical properties compared to normal concrete. This suggests that proper treatment of recycled aggregates and the strategic use of supplementary materials can effectively enhance the durability and strength of recycled aggregate concrete, making it a viable solution for sustainable construction.

Figure 16 demonstrates the relationship between the modulus of elasticity and the square root of compressive strength ($f_{cy}^{0.5}$) for various concrete mixes, comparing the results of the current study with established models and codes, including ACI 318, ACI 363, the Chinese code for recycled concrete, CEB-FIP, and Malaikah [77]-[81].The regression model derived from the current study, $E_C = 4833 * f_{cy}^{0.5}$, exhibits a strong correlation (R^2=0.9994), indicating excellent predictive accuracy for the modulus of elasticity based on the compressive strength of the concrete mixes.

Compared to existing models, the predictions from A.S. Malaikah (2003), the Chinese code for recycled concrete, and CEB-FIP are generally higher than the values observed in the current study. This difference may indicate that the modulus of elasticity achieved in the current study, while improved compared to untreated recycled aggregate concrete, remains slightly lower than the expectations of these codes and models. In contrast, the predictions of ACI 318 and ACI 363 are lower than the values from the current study, highlighting the enhanced stiffness achieved through the use of treated recycled aggregates and supplementary materials.

The comparison suggests that the treated recycled aggregate concrete used in this study performs well, though not to the level predicted by models such as A.S. Malaikah (2003) and the Chinese code. This could be attributed to inherent differences in aggregate properties, mix design, or experimental conditions. The findings emphasize the effectiveness of the adopted treatment method (0.1M hydrochloric acid) and mix optimization in improving the modulus of elasticity of recycled aggregate concrete, though further refinement may be needed to reach the performance levels anticipated by some established models.

Overall, the strong linear correlation between $f_{cy}^{0.5}$ and the modulus of elasticity reinforces the reliability of compressive strength as a predictor. While the current study does not exceed all predictions, it demonstrates the potential of treated recycled aggregates and supplementary materials to produce sustainable concrete with competitive mechanical properties, offering an environmentally friendly alternative to conventional concrete.

TABLE VI
MODULUS OF ELASTICITY TEST RESULTS

Mix Name	Compressive strength (fcy) (MPa)	Modulus of elasticity (Ec) (MPa)	Change percentage in modulus of elasticity (ΔEc) (%)
NC	43.0	32989	9.52
TRAC1	41.2	30122	0.00
TRAC2-SF10	45.6	33120	9.95
TRAC3-FA15	44.8	31654	5.09
TRAC4-KA5	43.7	31698	5.23

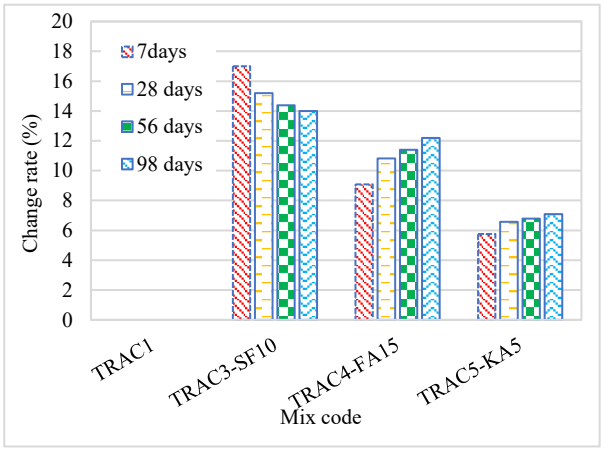

Fig. 14. Variations of compressive strength when compared with TRAC1.

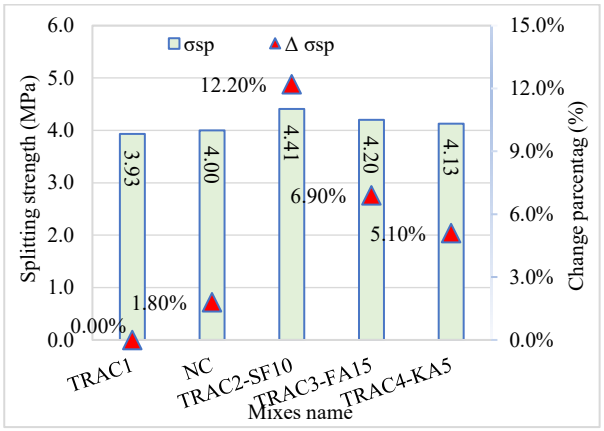

(a) Splitting strength values and percentage difference with respect to TRAC1

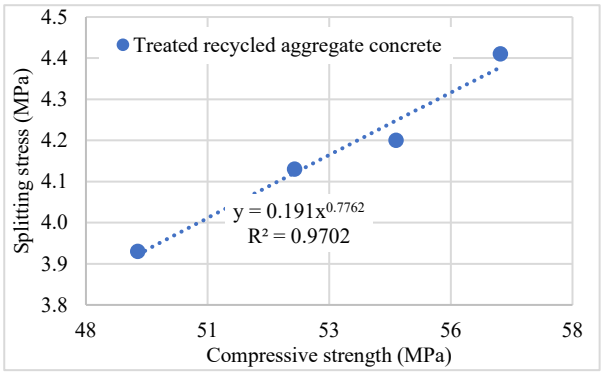

(b) Relationship between compressive strength and splitting tensile strength.

Fig. 15 Splitting strength test results and the relationship between compressive strength and splitting tensile strength.

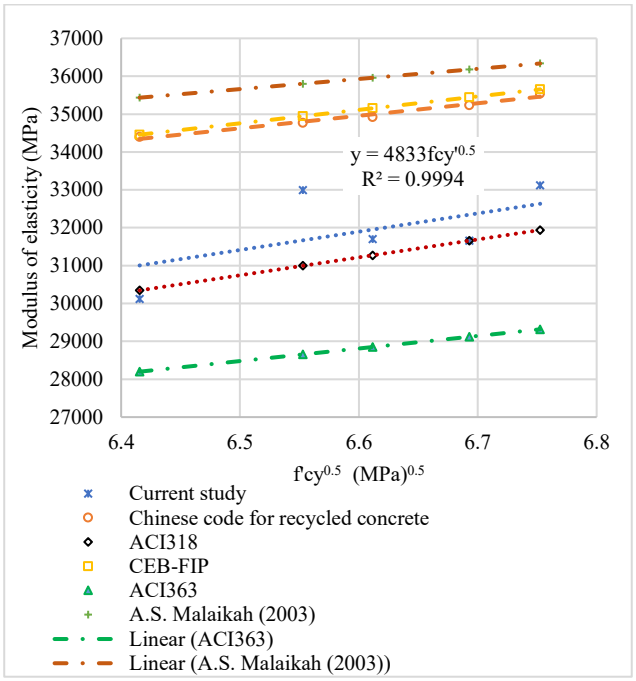

Fig. 16. Correlation results of several studies in respect of square roots of cylindrical compressive strength & modulus of elasticity. [77]-[80]

H. Flexural Strength

Figure 17 presents the flexural strength of various concrete mixes and the percentage change in flexural strength compared to the baseline mix, TRAC1, which uses 100% treated recycled aggregates. The baseline mix, TRAC1, records a flexural strength of 5.31 MPa, lower than the control mix, NC (6.01 MPa), which uses natural granite aggregates. This result indicates that despite the treatment process, recycled aggregates mixtures exhibit 13.1% lower flexural performance compared to natural aggregates mixtures. Among the mixes with supplementary cementitious materials (SCMs), TRAC2-SF10 (10% silica fume) demonstrates the most significant improvement, achieving a flexural strength of 6.09 MPa, which is 14.6% higher than TRAC1 and slightly surpasses NC by 1.3%. This indicates that silica fume is highly effective in enhancing the flexural performance of concrete with treated recycled aggregates.

Other modified mixes also show improvements over TRAC1, though to a lesser extent. TRAC3-FA15 (15% fly ash) achieves a flexural strength of 5.78 MPa, reflecting an 8.8% improvement compared to TRAC1. While not as effective as silica fume, fly ash still contributes to a noticeable enhancement in flexural strength. TRAC5-KA4, on the other hand, records the lowest flexural strength among the modified mixes at 5.58 MPa, with only a 5.0% increase relative to TRAC1, suggesting that the supplementary material used in this mix is less effective in improving the flexural properties of TRAC concrete.

Overall, the results underscore the inherent limitations of recycled aggregates in flexural performance compared to natural aggregates but also highlight the potential of SCMs to address these deficiencies. Silica fume, in particular, stands out as the most effective SCM, while fly ash provides moderate improvement. These findings emphasize the importance of optimizing mix designs with appropriate SCMs to enhance the mechanical properties of recycled aggregate

concrete and support its use in sustainable construction practices.

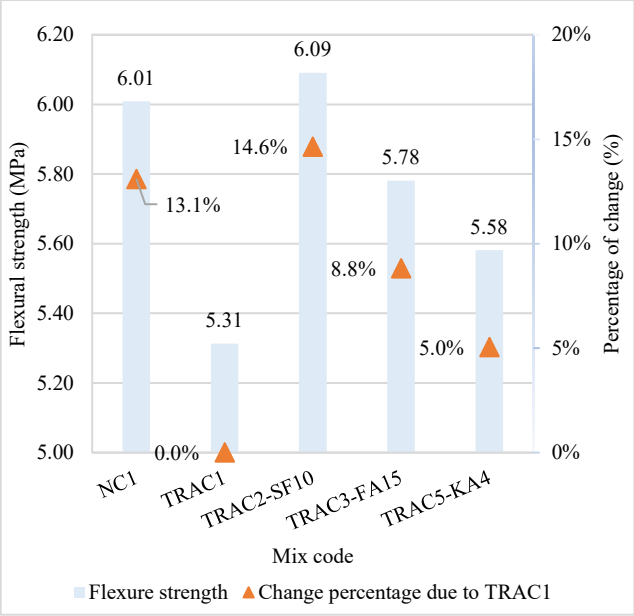

Fig. 17. The flexural strength and percentage difference respect to TRAC1.

I. Microstructure analysis.

Scanning Electron Microscopy (SEM) was employed to analyze and validate the microstructure of both TRAC1 and NC samples. The treatment applied to TRAC1 effectively removed most of the weak cement mortar and fine particles from the aggregate surface, resulting in a clean and rough texture, as shown in Figure 18(a). This clean and rough surface enhances the bond between the newly placed mortar and the old concrete aggregate, facilitating the propagation of hydration compounds, including calcium hydroxide (CH), calcium silicate hydrate (CSH), and ettringite (a hydrous calcium aluminum sulfate mineral.

The SEM image in Figure 18(b) illustrates the hydration products formed in TRAC1, such as CSH and CH. The inclusion of fly ash (FA), kaolin ash (KA), and silica fume (SF) as Supplementary Cementitious Materials (SCMs) significantly contributes to the microstructure. These SCMs, rich in reactive silicon dioxide, interact with CH produced during cement hydration to form additional CSH. This reaction fills voids and micro-cracks, thereby increasing the concrete's density and durability, as evidenced in Figures 18(c) and 18(d).

The SEM images reveal that the interaction between SCMs and CH leads to the formation of CSH, which strengthens the bond between the old interfacial transition zone (ITZ) and the new mortar. This process reduces porosity and improves the overall durability of TRAC compared to NC, resulting in a denser microstructure that is less prone to cracking. The presence of CSH and other hydration products confirms the effectiveness of SCMs in enhancing the microstructure, ultimately improving the mechanical properties and durability of the treated recycled concrete.

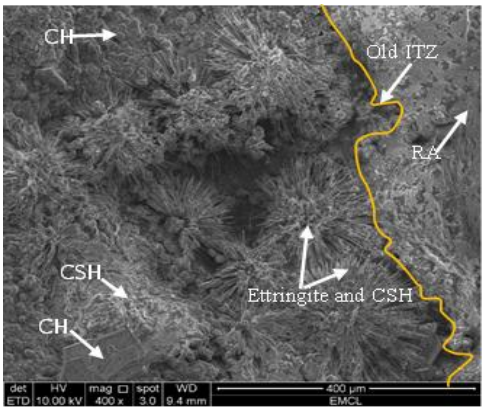

(a) SEM image shows cement mortar, old ITZ, and the rheology of aggregate and mortar.

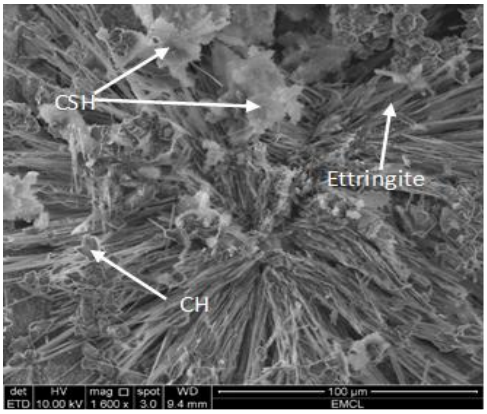

(b) SEM image confirms cement hydration component including mortar rheology.

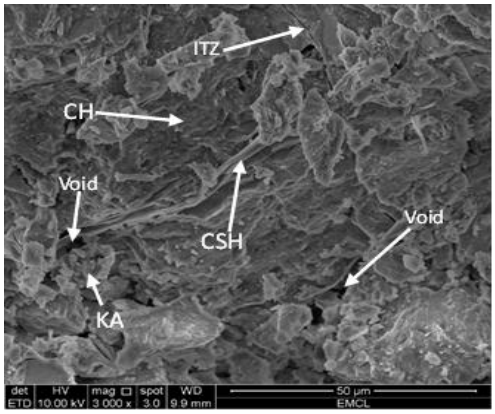

(c) SEM image illustrates cement hydration component, SCMs reaction, as well as mortar rheology.

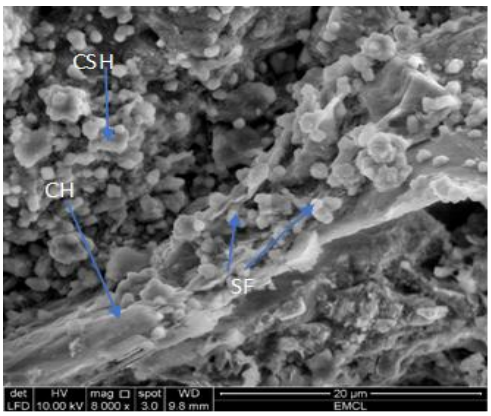

(d) The SEM image depicts cement hydration component in addition to SCMs reaction.

Fig. 18 SEM images for cement and SCMs Hydration component rheology.

IV. Conclusion

This study successfully demonstrated the potential of enhancing the properties of recycled aggregate concrete (RAC) through a combination of acid treatment, supplementary cementitious materials (SCMs), and the two-stage mixing approach (TSMA). The use of 0.1M hydrochloric acid (HCl) effectively improved the quality of recycled aggregates (RAs) by removing weak residual mortar, reducing water absorption, and enhancing aggregate surface roughness, which in turn strengthened the bond with the cement matrix. Incorporating SCMs such as silica fume (SF), fly ash (FA), and kaolin (KA) further enhanced the microstructure and mechanical properties of the treated recycled aggregate concrete (TRAC).

Concrete containing 10% SF showed the most significant improvements, with a 16.1% increase in compressive strength, a 14.6% improvement in flexural strength, and a 12.2% enhancement in splitting tensile strength. Additionally, the inclusion of SCMs reduced water absorption by up to 35.87%, porosity by 40.68%, and rapid chloride permeability by 73.41%, demonstrating substantial enhancements in durability. The study confirmed that SCMs react with calcium hydroxide (CH) to form additional calcium silicate hydrate (CSH), refining the interfacial transition zone (ITZ), filling micro-cracks, and reducing porosity.

Despite the challenges associated with fully replacing natural aggregates (NAs) with recycled aggregates (RAs), the combination of acid treatment, SCMs, and TSMA offers a viable and sustainable alternative to conventional concrete. This approach not only improves the mechanical and durability properties of RAC but also promotes environmental sustainability by reducing reliance on natural resources and minimizing construction waste.

Future research is recommended to explore hybrid combinations of SCMs and further optimize the treatment processes for RAs to achieve even greater performance improvements. The findings of this study underscore the potential of TRAC as a high-performance, eco-friendly solution for sustainable construction.

Credit author statement

Bassam Dabbour: Data Curation, Writing – Original Draft Preparation, Investigation **Mohd Zulham Affandi Mohd Zahid**: Writing – Reviewing and Editing **Badorul Hisham Abu Bakar**: Methodology and Supervision **Abrahem A Ali Blash**: Investigation **Noorhazlinda Abd Rahman**: Project Administration **Herni Halim**: Writing – Reviewing and Editing

Acknowledgement

The authors gratefully acknowledge Universiti Sains Malaysia for providing the raw materials for this research.

References

[1] S. Angel, "Urban expansion: theory, evidence and practice," 2023, Web Portal Ubiquity Press. doi: 10.5334/bc.348.

[2] N. Islam, M. Sandanayake, S. Muthukumaran, and D. Navaratna, "Review on Sustainable Construction and Demolition Waste Management—Challenges and Research Prospects," Apr. 01, 2024, Multidisciplinary Digital Publishing Institute (MDPI). doi: 10.3390/su16083289.

[3] C. M. Mah, T. Fujiwara, and C. S. Ho, "Construction and demolition waste generation rates for high-rise buildings in Malaysia," Waste Management and Research, vol. 34, no. 12, pp. 1224–1230, Dec. 2016, doi: 10.1177/0734242X16666944.

[4] J. Zhang, L. Ding, F. Li, and J. Peng, "Recycled aggregates from construction and demolition wastes as alternative filling materials for highway subgrades in China," J Clean Prod, vol. 255, May 2020, doi: 10.1016/j.jclepro.2020.120223.

[5] V. W. Y. Tam, M. Soomro, and A. C. J. Evangelista, "A review of recycled aggregate in concrete applications (2000–2017)," Constr Build Mater, vol. 172, pp. 272–292, May 2018, doi: 10.1016/j.conbuildmat.2018.03.240.

[6] C.-S. Poon and D. Chan, "The use of recycled aggregate in concrete in Hong Kong," Resour Conserv Recycl, vol. 50, no. 3, pp. 293–305, May 2007, doi: 10.1016/j.resconrec.2006.06.005.

[7] A. Katz, "Properties of concrete made with recycled aggregate from partially hydrated old concrete," Cem Concr Res, vol. 33, no. 5, pp. 703–711, May 2003, doi: 10.1016/S0008-8846(02)01033-5.

[8] R. Geyer, B. Kuczenski, T. Zink, and A. Henderson, "Common Misconceptions about Recycling," 2016, Blackwell Publishing. doi: 10.1111/jiec.12355.

[9] J. Kim, "Sustainable Construction Exploration: A Review of Multi-Recycling of Concrete Waste," Dec. 01, 2024, Springer Science and Business Media Deutschland GmbH. doi: 10.1007/s41742-024-00652-z.

[10] X. Ding, J. Hao, Z. Chen, J. Qi, and M. Marco, "New Mix Design Method for Recycled Concrete Using Mixed Source Concrete Coarse Aggregate," Waste Biomass Valorization, vol. 11, no. 10, pp. 5431–5443, Oct. 2020, doi: 10.1007/s12649-020-01073-7.

[11] B. Wang, L. Yan, Q. Fu, and B. Kasal, "A Comprehensive Review on Recycled Aggregate and Recycled Aggregate Concrete," Aug. 01, 2021, Elsevier B.V. doi: 10.1016/j.resconrec.2021.105565.

[12] J. Z. Xiao, J. B. Li, and C. Zhang, "On relationships between the mechanical properties of recycled aggregate concrete: An overview," Materials and Structures/Materiaux et Constructions, vol. 39, no. 6, pp. 655–664, 2006, doi: 10.1617/s11527-006-9093-0.

[13] Ali Babar, Ahmad Hawreen, Qureshi Liagat, Kurda Rawaz, and Hafez Hisham, "Enhancing the Hardened Properties of Recycled (RC) Concrete through ynergistic Incorporation of Fiber Reinforcement and Silica Fume," Materials, vol. 13, no. 4112, Sep. 2020, doi: 10.3390/ma13184112.

[14] A. Tanta, A. Kanoungo, S. Singh, and S. Kanoungo, "The effects of surface treatment methods on properties of recycled concrete aggregates," in Materials Today: Proceedings, Elsevier Ltd, 2021, pp. 1848–1852. doi: 10.1016/j.matpr.2021.09.223.

[15] E. Güneyisi, M. Gesoğlu, Z. Algin, and H. Yazici, "Effect of surface treatment methods on the properties of self-compacting concrete with recycled aggregates," Constr Build Mater, vol. 64, pp. 172–183, Aug. 2014, doi: 10.1016/j.conbuildmat.2014.04.090.

[16] Q. Peng, L. Wang, and Q. Lu, "Influence of recycled coarse aggregate replacement percentage on fatigue performance of recycled aggregate concrete," Constr Build Mater, vol. 169, pp. 347–353, Apr. 2018, doi: 10.1016/j.conbuildmat.2018.02.196.

[17] G. Bai, C. Zhu, C. Liu, and B. Liu, "An evaluation of the recycled aggregate characteristics and the recycled aggregate concrete mechanical properties," Apr. 20, 2020, Elsevier Ltd. doi: 10.1016/j.conbuildmat.2019.117978.

[18] C. Thomas, J. Setién, J. A. Polanco, P. Alaejos, and M. Sánchez De Juan, "Durability of recycled aggregate concrete," Constr Build Mater, vol. 40, pp. 1054–1065, 2013, doi: 10.1016/j.conbuildmat.2012.11.106.

[19] M. Marvila, P. de Matos, E. Rodríguez, S. N. Monteiro, and A. R. G. de Azevedo, "Recycled Aggregate: A Viable Solution for Sustainable Concrete Production," Aug. 01, 2022, MDPI. doi: 10.3390/ma15155276.

[20] J. M. Khatib, "Properties of concrete incorporating fine recycled aggregate," Cem Concr Res, vol. 35, no. 4, pp. 763–769, Apr. 2005, doi: 10.1016/j.cemconres.2004.06.017.

[21] M. Etxeberria, E. Vázquez, A. Marí, and M. Barra, "Influence of amount of recycled coarse aggregates and production process on properties of recycled aggregate concrete," Cem Concr Res, vol. 37, no. 5, pp. 735–742, May 2007, doi: 10.1016/j.cemconres.2007.02.002.

[22] S. Lotfi, M. Eggimann, E. Wagner, R. Mróz, and J. Deja, "Performance of recycled aggregate concrete based on a new concrete recycling technology," Constr Build Mater, vol. 95, pp. 243–256, Jul. 2015, doi: 10.1016/j.conbuildmat.2015.07.021.

[23] H. S. Joseph, T. Pachiappan, S. Avudaiappan, and E. I. S. Flores, "A Study on Mechanical and Microstructural Characteristics of Concrete Using Recycled Aggregate," Materials, vol. 15, no. 21, Nov. 2022, doi: 10.3390/ma15217535.

[24] J. Xiao, W. Li, and C. Poon, "Recent studies on mechanical properties of recycled aggregate concrete in China—A review," Sci China Technol Sci, vol. 55, no. 6, pp. 1463–1480, Jun. 2012, doi: 10.1007/s11431-012-4786-9.
[25] S.-C. Kou and C.-S. Poon, "Properties of concrete prepared with crushed fine stone, furnace bottom ash and fine recycled aggregate as fine aggregates," Constr Build Mater, vol. 23, no. 8, pp. 2877–2886, Aug. 2009, doi: 10.1016/j.conbuildmat.2009.02.009.
[26] K. Pandurangan, A. Dayanithy, and S. Om Prakash, "Influence of treatment methods on the bond strength of recycled aggregate concrete," Constr Build Mater, vol. 120, pp. 212–221, Sep. 2016, doi: 10.1016/j.conbuildmat.2016.05.093.
[27] J. Wang, J. Zhang, D. Cao, H. Dang, and B. Ding, "Comparison of recycled aggregate treatment methods on the performance for recycled concrete," Constr Build Mater, vol. 234, Feb. 2020, doi: 10.1016/j.conbuildmat.2019.117366.
[28] S. M. S. Kazmi, M. J. Munir, Y. F. Wu, I. Patnaikuni, Y. Zhou, and F. Xing, "Influence of different treatment methods on the mechanical behavior of recycled aggregate concrete: A comparative study," Cem Concr Compos, vol. 104, Nov. 2019, doi: 10.1016/j.cemconcomp.2019.103398.
[29] A. A. Bahraq, J. Jose, M. Shameem, and M. Maslehuddin, "A review on treatment techniques to improve the durability of recycled aggregate concrete: Enhancement mechanisms, performance and cost analysis," Sep. 01, 2022, Elsevier Ltd. doi: 10.1016/j.jobe.2022.104713.
[30] R. Wang, N. Yu, and Y. Li, "Methods for improving the microstructure of recycled concrete aggregate: A review," May 10, 2020, Elsevier Ltd. doi: 10.1016/j.conbuildmat.2020.118164.
[31] D. Marchon and R. J. Flatt, "Mechanisms of cement hydration," in Science and Technology of Concrete Admixtures, Elsevier Inc., 2016, pp. 129–145. doi: 10.1016/B978-0-08-100693-1.00008-4.
[32] H. M. Hamada et al., "Effect of silica fume on the properties of sustainable cement concrete," Journal of Materials Research and Technology, vol. 24, pp. 8887–8908, May 2023, doi: 10.1016/j.jmrt.2023.05.147.
[33] G. A. Rao, "Investigations on the performance of silica fume-incorporated cement pastes and mortars," Cem Concr Res, vol. 33, no. 11, pp. 1765–1770, Nov. 2003, doi: 10.1016/S0008-8846(03)00171-6.
[34] V. W.-Y. Tam, X.-F. Gao, and C. M. Tam, "Comparing performance of modified two-stage mixing approach for producing recycled aggregate concrete," Magazine of Concrete Research, vol. 58, no. 7, pp. 477–484, Sep. 2006, doi: 10.1680/macr.2006.58.7.477.
[35] M. Bhattacharya and K. V. Harish, "An integrated approach for studying the hydration of portland cement systems containing silica fume," Constr Build Mater, vol. 188, pp. 1179–1192, Nov. 2018, doi: 10.1016/j.conbuildmat.2018.08.114.
[36] V. W. Y. Tam, C. M. Tam, and Y. Wang, "Optimization on proportion for recycled aggregate in concrete using two-stage mixing approach," Constr Build Mater, vol. 21, no. 10, pp. 1928–1939, Oct. 2007, doi: 10.1016/j.conbuildmat.2006.05.040.
[37] V. W. Y. Tam, X. F. Gao, and C. M. Tam, "Microstructural analysis of recycled aggregate concrete produced from two-stage mixing approach," Cem Concr Res, vol. 35, no. 6, pp. 1195–1203, Jun. 2005, doi: 10.1016/j.cemconres.2004.10.025.
[38] V. W. Y. Tam and C. M. Tam, "Diversifying two-stage mixing approach (TSMA) for recycled aggregate concrete: TSMAs and TSMAsc," Constr Build Mater, vol. 22, no. 10, pp. 2068–2077, Oct. 2008, doi: 10.1016/j.conbuildmat.2007.07.024.
[39] J. Vengadesh Marshall Raman and V. Ramasamy, "Various treatment techniques involved to enhance the recycled coarse aggregate in concrete: A review," in Materials Today: Proceedings, Elsevier Ltd, 2020, pp. 6356–6363. doi: 10.1016/j.matpr.2020.10.935.
[40] P. Saravanakumar, K. Abhiram, and B. Manoj, "Properties of treated recycled aggregates and its influence on concrete strength characteristics," Constr Build Mater, vol. 111, pp. 611–617, May 2016, doi: 10.1016/j.conbuildmat.2016.02.064.
[41] Aleksandar Radević, Iva Despotović, Dimitrije Zakić, Marko Orešković, and Dragica Jevtić, "INFLUENCE OF ACID TREATMENT AND CARBONATION ON THE PROPERTIES OF RECYCLED CONCRETE AGGREGATE," Chemical Industry and Chemical Engineering Quarterly, vol. 24, no. 1, pp. 23–30, 2008.
[42] R. Huo, S. Li, and Y. Ding, "Experimental Study on Physicochemical and Mechanical Properties of Mortar Subjected to Acid Corrosion," Advances in Materials Science and Engineering, vol. 2018, Jun. 2018, doi: 10.1155/2018/3283907.
[43] J. Duchesne and A. Bertron, "Leaching of cementitious materials by pure water and strong acids (HCl and HNO3)," RILEM State-of-the-Art Reports, vol. 10, pp. 91–112, 2013, doi: 10.1007/978-94-007-5413-3_4.
[44] Y. Tam, X.-F. Gao, and C. M. Tam, "Comparing performance of modified two-stage mixing approach for producing recycled aggregate concrete," Magazine of Concrete Research, vol. 58, no. 7, pp. 477–484, Sep. 2006, [Online]. Available: www.concrete-research.com
[45] Wu Zemei, Khayat H. Kamal, and Shi Caijun, "Changes in rheology and mechanical prop...ance concrete with silica fume content," Cem Concr Res, vol. 123, no. 105786, Jun. 2019.
[46] Jagan S and Neelakantan R. T., "Effect of silica fume on the hardened and durability properties of concrete," International Review of Applied Science and Engineering, pp. 44–49, 2021.
[47] Kansal Mohan Chander and Goyal Rajesh, "Analysing mechanical properties of concrete with nano silica, silica fume and steel slag," Material Today, vol. 45, pp. 4520–4525, 2021.
[48] J. Gražulytė, A. Vaitkus, O. Šernas, and D. Čygas, "Effect of silica fume on high-strength concrete performance," in 5th World Congress on Civil, Structural, and Environmental Engineering (CSEE'20), 2020, pp. 1–6.
[49] Nagrockiene D, Rutkauskas A, Pundiene I, and Girniene I, "The Effect of Silica Fume Addition on the Resistance of Concrete to Alkali Silica Reaction," in Materials Science and Engineering, 2019.
[50] S. Sahoo, P. K. Parhi, and B. Chandra Panda, "Durability properties of concrete with silica fume and rice husk ash," Clean Eng Technol, vol. 2, Jun. 2021, doi: 10.1016/j.clet.2021.100067.
[51] Sahoo Smita, Parhi kumar Pravat, and Panda Ghandra Bikash, "Durability properties of concrete with silica fume and husk ash," Clear Engineering Technology 2, vol. 48, pp. 1789–1795, Mar. 2021, Accessed: Mar. 16, 2024. [Online]. Available: https://doi.org/10.1016/j.matpr.2021.08.347
[52] S. Joel, "Compressive strength of concrete using fly ash and rice husk ash: A review," Civil Engineering Journal (Iran), vol. 6, no. 7, pp. 1400–1410, Jul. 2020, doi: 10.28991/cej-2020-03091556.
[53] A. A. Phul, M. J. Memon, S. N. R. Shah, and A. R. Sandhu, "GGBS And Fly Ash Effects on Compressive Strength by Partial Replacement of Cement Concrete," Civil Engineering Journal, vol. 5, no. 4, pp. 913–921, Apr. 2019, doi: 10.28991/cej-2019-03091299.
[54] P. Kara De Maeijer et al., "Effect of ultra-fine fly ash on concrete performance and durability," Constr Build Mater, vol. 263, Dec. 2020, doi: 10.1016/j.conbuildmat.2020.120493.
[55] Y. Fan, S. Zhang, S. Kawashima, and S. P. Shah, "Influence of kaolinite clay on the chloride diffusion property of cement-based materials," Cem Concr Compos, vol. 45, pp. 117–124, 2014, doi: 10.1016/j.cemconcomp.2013.09.021.
[56] Krivenko P. and Petropavlovskyi O., "A comparative study on the influence of metakaolin and kaolin additives on properties and structure of the alkali-activated slag cement and concrete," Eastern-European Journal of Enterprise Technologies, vol. 91, no. 1729–3774, pp. 33–39, 2018, doi: 10.15587/1729-4061.2018.119624.
[57] S. Abdallah, M. Fan, and D. Rees, "Bonding Mechanisms and Strength of Steel Fiber–Reinforced Cementitious Composites: Overview," Journal of Materials in Civil Engineering, vol. 30, no. 3, Jan. 2018.
[58] Kararas Mehmet, Benli Ahmet, and Arslan Furkan, "The effects of kaolin and calcined kaolin on the durability and mechanical properties of self compacting mortars subjected to high temperatures," Constr Build Mater, vol. 265, no. 950–0618, pp. 300–312, Aug. 2020.
[59] D. E. Dixon et al., "Standard Practice for Selecting Proportions for Normal, Heavyweight, and Mass Concrete (ACI 211.1-91) Chairman, Subcommittee A," 1991.
[60] A. International and files indexed by mero, "Standard Test Method for Flexural Strength of Concrete (Using Simple Beam with Third-Point Loading) 1," ASTM C78-22, Mar. 2022. doi: 10.1520/C0078_C0078M-22.
[61] ASTM International, Standard Test Method for Flexural Toughness and First-Crack Strength of Fiber-Reinforced Concrete (Using Beam With Third-Point Loading), vol. 04.02. ASTM C1018-17, 2017.
[62] ASTM INTERNATIONAL, Standard Test Method for Electrical Indication of Concrete's Ability to Resist Chloride Ion Penetration, ASTM C1202-22E1., vol. 04.02. 2020. doi: 10.1520/C1202-22E01.
[63] ASTM International, Standard Practice for Making and Curing Concrete Test Specimens in the Laboratory, vol. 04.02. ASTM C 192-19, 2020. doi: 10.1520/C0192_C0192M-19.
[64] British Standards Institution, Testing concrete. Part 102 Method for determination of slump. 1998.
[65] ASTM International, Standard Test Method for Slump of Hydraulic-Cement Concrete, vol. 04.02. ASTM C 143-20, 2020. doi: 10.1520/C0143_C0143M-20.
[66] ASTM International, Standard Test Method for Density, Absorption, and Voids in Hardened Concrete, ASTM International., vol. 04.02. ASTM C642-21, 2022. doi: 10.1520/C0642-21.
[67] J. G. Cabrera and C. J. Lynsdale, "A new gas permeameter for measuring the permeability of mortar and concrete," 1988.

[68] X. Liu, K. S. Chia, and M.-H. Zhang, "Water absorption, permeability, and resistance to chloride-ion penetration of lightweight aggregate concrete," Constr Build Mater, vol. 25, no. 1, pp. 335–343, 2011, doi: https://doi.org/10.1016/j.conbuildmat.2010.06.020.
[69] ACI Committee 116, "Method for determination of cube compressive strength," vol. BS 1881: part 116, 1983.
[70] ASTM International, Splitting Tensile Strength of Cylindrical Concrete Specimens, vol. 04.02. ASTM 496-17, 2017. doi: 10.1520/C0496_C0496M-17.
[71] ASTM International, Standard Test Method for Static Modulus of Elasticity and Poisson's Ratio of Concrete in Compression, vol. 04.02. ASTM C496-22, 2022. doi: 10.1520/C0469_C0469M-22.
[72] M. Amin, A. M. Zeyad, B. A. Tayeh, and I. Saad Agwa, "Effect of ferrosilicon and silica fume on mechanical, durability, and microstructure characteristics of ultra high-performance concrete," Constr Build Mater, vol. 320, Feb. 2022, doi: 10.1016/j.conbuildmat.2021.126233.
[73] A. Habibi, A. M. Ramezanianpour, M. Mahdikhani, and O. Bamshad, "RSM-based evaluation of mechanical and durability properties of recycled aggregate concrete containing GGBFS and silica fume," Constr Build Mater, vol. 270, Feb. 2021, doi: 10.1016/j.conbuildmat.2020.121431.
[74] K. Ali, M. I. Qureshi, S. Saleem, and S. U. Khan, "Effect of waste electronic plastic and silica fume on mechanical properties and thermal performance of concrete," Constr Build Mater, vol. 285, May 2021, doi: 10.1016/j.conbuildmat.2021.122952.
[75] F. Köksal, F. Altun, I. Yiğit, and Y. Şahin, "Combined effect of silica fume and steel fiber on the mechanical properties of high strength concretes," Constr Build Mater, vol. 22, no. 8, pp. 1874–1880, Aug. 2008, doi: 10.1016/j.conbuildmat.2007.04.017.
[76] A. M. Falmata, A. Sulaiman, R. N. Mohamed, and A. U. Shettima, "Mechanical properties of self-compacting high-performance concrete with fly ash and silica fume," SN Appl Sci, vol. 2, no. 1, Jan. 2020, doi: 10.1007/s42452-019-1746-z.
[77] A. F. Hashmi, M. Shariq, and A. Baqi, "An investigation into age-dependent strength, elastic modulus and deflection of low calcium fly ash concrete for sustainable construction," Constr Build Mater, vol. 283, May 2021, doi: 10.1016/j.conbuildmat.2021.122772.
[78] A. Lotfy, O. Karahan, E. Ozbay, K. M. A. Hossain, and M. Lachemi, "Effect of kaolin waste content on the properties of normal-weight concretes," Constr Build Mater, vol. 83, pp. 102–107, May 2015, doi: 10.1016/j.conbuildmat.2015.03.002.
[79] Z. Çelik, A. F. Bingöl, and A. S. Ağsu, "Fresh, mechanical, sorptivity and rapid chloride permeability properties of self-compacting concrete with silica fume and fly ash," Iranian Journal of Science and Technology - Transactions of Civil Engineering, vol. 46, no. 2, pp. 789–799, Apr. 2022, doi: 10.1007/s40996-021-00676-x.
[80] T. Yunchao, C. Zheng, F. Wanhui, N. Yumei, L. Cong, and C. Jieming, "Combined effects of nano-silica and silica fume on the mechanical behavior of recycled aggregate concrete," Nanotechnol Rev, vol. 10, no. 1, pp. 819–838, Jan. 2021, doi: 10.1515/ntrev-2021-0058.
[81] M. Alamri et al., "Enhancing the engineering characteristics of sustainable recycled aggregate concrete using fly ash, metakaolin and silica fume," Heliyon, vol. 10, no. 7, Apr. 2024, doi: 10.1016/j.heliyon.2024.e29014.
[82] ACI Committee 318. and American Concrete Institute., Building code requirements for structural concrete (ACI 318-11) and commentary. American Concrete Institute, 2011.
[83] ACI Committee 363, "State-of-the-Art Report on High-Strength Concrete," 1997.
[84] A. S. Malaikah, "A Proposed Relationship for the Modulus of Elasticity of High Strength Concrete Using Local Materials in Riyadh," King Saud Univ, vol. 17, no. 2, pp. 131–142, 2004.
[85] K. Li, C. Zhou, and Z. Chen, Chinese code for durability design of concrete structures: A state-of-art report. 2008.
[86] CEB-FIP Model Code, Model Code for Concrete 1998, vol. 1. London: Thomas Telford Services Ltd, 1998.
[87] J. Chen, Y. Zhou, and F. Yin, "A Practical Equation for the Elastic Modulus of Recycled Aggregate Concrete," Buildings, vol. 12, no. 2, Feb. 2022, doi: 10.3390/buildings12020187.